Modeling the Elastic Support Properties of Bernoulli-Euler Beams

T.A.N. Silva[1,2], **N.M.M. Maia**[2]

[1] Department of Mechanical Engineering, Instituto Superior de Engenharia de Lisboa
Rua Conselheiro Emídio Navarro, 1, 1959-007 Lisboa, Portugal
E-mail: tasilva@dem.isel.ipl.pt

[2] Department of Mechanical Engineering, Instituto Superior Técnico
Av. Rovisco Pais, 1, 1049-001 Lisboa, Portugal
E-mail: nmaia@dem.ist.utl.pt

ABSTRACT

Considering the transverse vibration problem of a machine rotor, the authors deal with the free vibration of elastically restrained Bernoulli-Euler beams. Based upon Rayleigh's quotient, an iterative strategy is developed to identify the approximated torsional stiffness coefficients, which allows to bringing together experimental results obtained through impact tests and the ones of the theoretical model. The proposed algorithm treats the vibration of continuous beams taking into account different stiffness coefficients at the left end side and intermediate supports and the effect of attached mass with inertia at the free beam tip, not just on the energetic terms of the Rayleigh's quotient but also on the mode shapes, considering the shape functions defined in branches. A number of loading cases are studied and examples are given to illustrate the validity of the model and the accuracy of the obtained natural frequencies.

KEYWORDS: Transverse vibration of beams; Elastic supports; Torsional stiffness coefficients.

1   INTRODUCTION

The study of beam-like components that present cross section variations along the length and carry concentrated masses and/or springs is often addressed by means of approximated numerical methods, like Rayleigh's quotient. The accuracy of such an approach depends on the chosen shape function, according to Rayleigh's theorem [1]. Figure 1 shows the physical system under consideration, a rotor with a disc at the right end side. The objective of the present work is to develop an accurate model of the system in order to replicate the experimental natural frequencies in lateral bending.

While the rotor itself presents no problem and can easily be studied as a Bernoulli-Euler beam with a concentrated mass, the identification of the adequate torsional and linear stiffness properties associated to the end supports remains a challenge. In a similar context, De Rosa et al. [2] suppose the beam elastically restrained against rotation and translation at both ends, so that it is possible to study all the common boundary conditions. Those authors show that trigonometric functions work slightly better than the static deflections and highlight the accuracy of Rayleigh's quotient to the true frequencies. References [3-6] present exact solutions for the frequency equation of a Bernoulli-Euler beam restricting the stiffness coefficients, in order to reproduce some particular cases, and accounting for the rotation inertia of attached discs and their eccentricity. Similar problems are treated in [7, 8], with intermediate supports. Wu and Chen [9] studied the bending vibrations of wedge Bernoulli-Euler beams with any number of point masses, verifying that the mass distribution on the beam affects the dynamical behavior more than the mass addition itself. The works of Biondi and Caddemi [10, 11] treat beams with
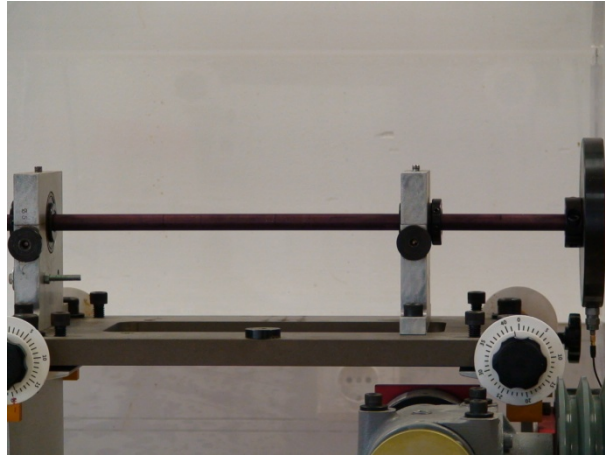
Figure 1: System under study (MFS, SpectraQuest, Inc.).

discontinuities in the curvature or in the slope functions, allowing the adoption of different materials or different cross sections in the model. Elishakoff and Pentaras [12] worked on the free vibration of non-homogeneous Bernoulli-Euler beams using a polynomial approach for the mode shape of the natural frequency of interest. The developed formulation does not require numerical tackle and provides a useful tool to the design phase. The above referred papers deal with slender beams, verifying $\ell / D > 10$. As a consequence, the inertial rotation energy of an infinitesimal element *dx* is negligible compared to its translational energy, justifying the applicability of the Bernoulli-Euler beam theory. Sometimes, when this principle is violated, the problem has to be treated using Timoshenko beam theory [13-15].

In the present work one shall use Rayleigh's quotient, with shape functions that have into account the torsional flexibility of the supports, while assuming infinite rigidity along the vertical direction (figure 2). The algorithm will also include the effect of the mass and torsional inertia of the attached disc. Such an approach aims at a more precise model that reproduces better the real dynamic behavior of the system, rather than assuming simply supported or perfectly clamped ends. After showing that the simply supported case is not the best way to model the physical system, the updating procedure for identifying the value of the torsional stiffness of both supports will be explained.
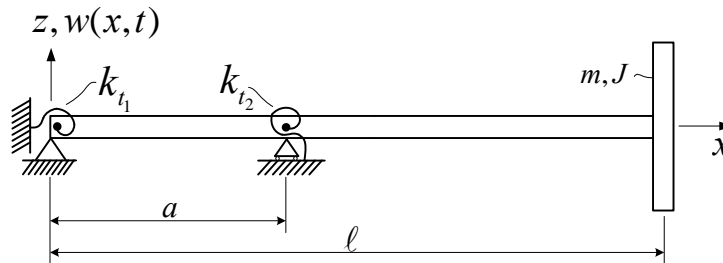

Figure 2: Model of a beam with elastic torsional supports and a rigid disc at $x = \ell$.

2 THEORETICAL BACKGROUND

To obtain an analytical model that reproduces the physical system (figure 1) one considers the Rayleigh's quotient, using the Bernoulli-Euler beam theory to define the shape functions. On a first attempt one tries the simply supported (SS) case. However, the results for this ideal case differ from the experimental ones, especially for the second natural frequency. Therefore, one proposes to build a model considering that the supports of the beam present different torsional stiffnesses k_{t_i} (elastic supports - ES), whose values are iterated until the error between experimental and numerical results satisfies a given tolerance τ.

Regarding Rayleigh's method, the energy dissipation is neglected and therefore the Principle of Conservation of Energy holds:

$$\Delta(T+V) = 0 \quad \Rightarrow \quad T_{\max} = V_{\max} \tag{1}$$

where T and V are the kinetic and potential energies, respectively.

Through the quantification of the work performed by the elastic forces, in relation to the equilibrium position of the beam, the potential energy is

$$V = \frac{1}{2}\int_0^\ell M(x,t)d\theta \tag{2}$$

where $M(x,t)$ is the bending moment given by $M(x,t) = E(x)I(x)\partial^2 w(x,t)/\partial x^2$, ℓ is the length of the beam and θ is the rotation angle given by $\theta(x,t) = \partial w(x,t)/\partial x$. $E(x)$ is the Young modulus and $I(x)$ the second moment of area of the beam; $w(x,t)$ represents the lateral displacement of the beam in relation to its equilibrium position.

Under undamped free vibration conditions, the time variation of $w(x,t)$ can be shown to be harmonic and therefore the displacement response is given by the harmonic variation of a shape function $\phi(x)$:

$$w(x,t) = \phi(x)\sin(\omega t + \varphi) \tag{3}$$

As $w(x,t)_{\max} = \phi(x)$, it follows that

$$V_{\max} = \frac{1}{2}\int_0^\ell E(x)I(x)\left(\frac{d^2\phi(x)}{dx^2}\right)^2 dx \tag{4}$$

On the other hand, the kinetic energy is given by

$$T = \frac{1}{2}\int_0^\ell \dot{w}(x,t)^2 dm \tag{5}$$

From (3), $\dot{w}(x,t)_{\max} = \omega\,\phi(x)$. As $dm = \rho(x)A(x)dx$, where $\rho(x)$ is the density of the material and $A(x)$ the cross sectional area of the beam, one has

$$T_{\max} = \omega^2\frac{1}{2}\int_0^\ell \rho(x)A(x)\phi^2(x)dx \tag{6}$$

2.1 Rayleigh's quotient

Rayleigh's quotient, R, results from the application of (1) and therefore, for a beam with no extra masses and springs, equating (4) and (6) leads to

$$R = \omega^2 = \frac{\int_0^\ell E(x)I(x)\left(\phi''(x)\right)^2 dx}{\int_0^\ell \rho(x)A(x)\phi^2(x)dx} \tag{7}$$

where prime denotes differentiation with respect to the spatial coordinate x.

Rayleigh's quotient has several interesting properties from the numerical point of view. One of them is the upper bound approximation for the natural frequency value, as long as one provides a shape function $\phi(x)$ close enough to the true mode shape, respecting at least the geometric boundary conditions of the problem. As a first order variation on $\phi(x)$ corresponds to a second order variation on ω^2, Rayleigh's quotient has a stationary value (a

minimum in this case) in the neighborhood of the true mode shape. This is verified not only for the fundamental natural frequency, but for all of them, i.e., a good approximation for the nth shape function $\phi_n(x)$ leads to a good approximation for the nth natural frequency ω_n.

Taking into account the possible existence of concentrated parameters along the length of the beam, such as springs and masses (and corresponding inertias), one can rewrite (4) and (6). Therefore, the total maximum value for the potential energy will be given by

$$V_{max} = V_b + \sum_i V_{k_i} + \sum_j V_{k_{t_j}} \tag{8}$$

where V_b is the potential energy of the beam itself, given by (4), and

$$V_{k_i} = \frac{1}{2} k_i \, \phi_n^2(x_i) \ , \ V_{k_{t_j}} = \frac{1}{2} k_{t_j} \, \phi_n'(x)\Big|_{x=x_j}^2 \tag{9}$$

are the potential energies of each local translational and torsional stiffnesses k_i and k_{t_j}, respectively.

The maximum kinetic energy will be given by

$$T_{max} = T_b + \sum_r T_{m_r} + \sum_s T_{J_s} \tag{10}$$

where T_b is the kinetic energy of the beam itself, given by (6), and

$$T_{m_r} = \frac{1}{2} \omega^2 m_r \, \phi_n^2(x_r) \ , \ T_{J_s} = \frac{1}{2} \omega^2 J_s \, \phi_n'(x)\Big|_{x=x_s}^2 \tag{11}$$

are the kinetic energies of each local mass m_r and inertia J_s, respectively.

Hence, Rayleigh's quotient applied to a general case, will be defined as

$$R = \omega_n^2 = \frac{\int_0^\ell E(x)I(x)\left(\phi_n''(x)\right)^2 dx + \sum_i k_i \, \phi_n^2(x_i) + \sum_j k_{t_j} \, \phi_n'(x)\Big|_{x=x_j}^2}{\int_0^\ell \rho(x)A(x)\phi_n^2(x)\,dx + \sum_r m_r \, \phi_n^2(x_r) + \sum_s J_s \, \phi_n'(x)\Big|_{x=x_s}^2} \tag{12}$$

Note that in our case study, the beam is uniform and the translational springs have infinite stiffnesses. Thus,

$$R = \omega_n^2 = \frac{EI\int_0^\ell \left(\phi_n''(x)\right)^2 dx + \sum_j k_{t_j} \, \phi_n'(x)\Big|_{x=x_j}^2}{\rho A\int_0^\ell \phi_n^2(x)\,dx + \sum_r m_r \, \phi_n^2(x_r) + \sum_s J_s \, \phi_n'(x)\Big|_{x=x_s}^2} \tag{13}$$

2.2   Shape functions

In Rayleigh's quotient the selection of the shape function may have a significant impact on the solution of the problem. The question is how to choose such an appropriate shape function. This should at least verify the geometric boundary conditions, although more accurate results are expected if it verifies the natural boundary conditions too. Moreover, it is also known that, in general, trigonometric functions provide better results than polynomial functions or functions based upon static deflections. Certainly a good choice would be to take the shape function that results from the solution of the equilibrium equation of the Bernoulli-Euler beam with uniform material and cross section in free vibration:

$$c^2 \frac{\partial^4 w(x,t)}{\partial x^4} + \frac{\partial^2 w(x,t)}{\partial t^2} = 0 \tag{14}$$

where $c^2 = (EI)/(\rho A)$ and $w(x,t) = \phi(x)T(t)$; the shape function $\phi(x)$ is given by

$$\phi(x) = C_1 \sin(\beta x) + C_2 \cos(\beta x) + C_3 \sinh(\beta x) + C_4 \cosh(\beta x) \tag{15}$$

where '*C*' are constants and *β* is related to the natural frequency through $\omega_n = (\beta_n \ell)^2 \sqrt{(EI)/(\rho A \ell^4)}$. Applying the set of boundary conditions to (15) leads to an eigenproblem, whose eigenvalues are $\beta_n \ell$ ($n = 1, \dots \infty$) and whose eigenvectors are constituted by the constants '*C*'. From the eigenvalues, the natural frequencies are calculated and, from the eigenvectors, the mode shapes are defined as a function of the eigenvalues, as

$$\phi_n(x) = C_1^{(n)} \sin(\beta_n x) + C_2^{(n)} \cos(\beta_n x) + C_3^{(n)} \sinh(\beta_n x) + C_4^{(n)} \cosh(\beta_n x) \tag{16}$$

For the problem under study (figures 1 and 2), several sets of boundary conditions were assumed in order to reproduce the physical system conditions. As one considers an intermediate support at *x=a*, one must complement the boundary conditions with the correspondent continuity equations. As a result, $\phi(x)$ should be defined as a piecewise function, as follows:

$$\phi_n(x) = \begin{cases} \{\phi_n(x)\}_1 & \text{for } x \in [0, a] \\ \{\phi_n(x)\}_2 & \text{for } x \in [a, \ell] \end{cases} \tag{17}$$

with

$$\{\phi_n(x)\}_1 = C_1^{(n)} \sin(\beta_n x) + C_2^{(n)} \cos(\beta_n x) + C_3^{(n)} \sinh(\beta_n x) + C_4^{(n)} \cosh(\beta_n x) \tag{18}$$

$$\{\phi_n(x)\}_2 = C_5^{(n)} \sin(\beta_n x) + C_6^{(n)} \cos(\beta_n x) + C_7^{(n)} \sinh(\beta_n x) + C_8^{(n)} \cosh(\beta_n x) \tag{19}$$

In the next sub-sections the considered sets of boundary conditions and continuity equations are described.

2.2.1   Simply supported beam (SS)

To reproduce this ideal case one assumes $k_i = \infty \wedge k_{t_j} = 0$ for both beam supports, placed at $x = 0 \wedge x = a$, which leads us to the following set of boundary conditions:

$$w(0,t) = \left.\frac{\partial^2 w(x,t)}{\partial x^2}\right|_{x=0} = 0 \tag{20}$$

$$\left.\frac{\partial^2 w(x,t)}{\partial x^2}\right|_{x=\ell} = \left.\frac{\partial^3 w(x,t)}{\partial x^3}\right|_{x=\ell} = 0 \tag{21}$$

and continuity equations:

$$\left.\{\phi_n(x)\}_1\right|_{x=a} = \left.\{\phi_n(x)\}_2\right|_{x=a} = 0 \tag{22}$$

$$\left.\{\phi_n'(x)\}_1\right|_{x=a} = \left.\{\phi_n'(x)\}_2\right|_{x=a} \tag{23}$$

$$\left.\{\phi_n''(x)\}_1\right|_{x=a} = \left.\{\phi_n''(x)\}_2\right|_{x=a} \tag{24}$$

2.2.2 Beam on elastic supports (ES)

Considering a more realistic approach, the proposed model consists of a solution with a beam on elastic supports (ES) carrying a disc at its free end. The expression "elastic support" designates a support where $k_i = \infty \wedge k_{t_j} > 0$ with the boundary conditions given by:

$$w(0,t) = 0 \tag{25}$$

$$EI\left.\frac{\partial^2 w(x,t)}{\partial x^2}\right|_{x=0} = k_{t_1}\left.\frac{\partial w(x,t)}{\partial x}\right|_{x=0} \tag{26}$$

$$EI\left.\frac{\partial^2 w(x,t)}{\partial x^2}\right|_{x=\ell} = -J_s\left.\frac{\partial^3 w(x,t)}{\partial x\,\partial t^2}\right|_{x=\ell} \tag{27}$$

$$EI\left.\frac{\partial^3 w(x,t)}{\partial x^3}\right|_{x=\ell} = m_r\left.\frac{\partial^2 w(x,t)}{\partial t^2}\right|_{x=\ell} \tag{28}$$

and continuity equations:

$$\left\{\phi_n(x)\right\}_1\big|_{x=a} = \left\{\phi_n(x)\right\}_2\big|_{x=a} = 0 \tag{29}$$

$$\left\{\phi_n'(x)\right\}_1\big|_{x=a} = \left\{\phi_n'(x)\right\}_2\big|_{x=a} \tag{30}$$

$$\left\{\phi_n''(x)\right\}_1\big|_{x=a} - k_{t_2}\left\{\phi_n'(x)\right\}_1\big|_{x=a} = \left\{\phi_n''(x)\right\}_2\big|_{x=a} \tag{31}$$

Note that for this case we consider two configurations:

- **Beam on elastic supports (ES1)** with $k_{t_1} = k_{t_2}$;
- **Beam on elastic supports (ES2)** with $k_{t_1} \neq k_{t_2}$.

3 NUMERICAL PROCEDURE

With the purpose of identifying the elastic properties of the beam supports, a numerical procedure has been developed, bearing in mind the reconciliation between the numerical results for the first natural frequency and the experimental ones ($\omega_1|_{EXP}$). To start this updating procedure, one assumes as a first approximation the solutions for a simply supported case (SS), $\beta_1\ell|_{SS}$ and $\phi_1(x)|_{SS}$. From (13) and for iteration $p=1$, the torsional stiffness coefficients are given by:

$$k_{t_1}^{(1)} = k_{t_2}^{(1)} = \frac{\omega_1^2\big|_{EXP}\left(\rho A\int_0^\ell \phi_1(x)\big|_{SS}^2\,dx + m\left\{\phi_1(x)\right\}_2^2\big|_{SS\,@\,x=\ell} + J\left\{\phi_1(x)\right\}_2^2\big|_{SS\,@\,x=\ell}\right) - EI\int_0^\ell \phi_1''(x)\big|_{SS}^2\,dx}{\left\{\phi_1(x)\right\}_1^2\big|_{SS\,@\,x=0} + \left\{\phi_1(x)\right\}_1^2\big|_{SS\,@\,x=a}} \tag{32}$$

In an iterative scheme, one shall use the solutions for a beam on elastic supports, $\beta_1\ell|_{ES}$ and $\phi_1(x)|_{ES}$, calculating, when required, different stiffness coefficients k_{t_1} and k_{t_2}, as follows:

Step 1. with $\beta_1\ell\big|_{ES}$ and $\phi_1(x)\big|_{ES}$ as function of $k_{t_1}{}^{(p)}$ and $k_{t_2}{}^{(p)}$, compute $k_{t_1}{}^{(p+1)}$:

$$k_{t_1}{}^{(p+1)} = \frac{\omega_1^2\big|_{EXP}\left(\rho A\int_0^\ell \phi_1(x)\big|_{ES}^2 dx + m\{\phi_1(x)\}_2^2\big|_{ES\,@\,x=\ell} + J\{\phi_1'(x)\}_2^2\big|_{ES\,@\,x=\ell}\right) - \left(EI\int_0^\ell \phi_1''(x)\big|_{ES}^2 dx + k_{t_2}{}^{(p)}\{\phi_1'(x)\}_1^2\big|_{ES\,@\,x=a}\right)}{\{\phi_1'(x)\}_1^2\big|_{ES\,@\,x=0}} \tag{33}$$

Step 2. similarly, with $\beta_1\ell\big|_{ES}$ and $\phi_1(x)\big|_{ES}$ as function of $k_{t_1}{}^{(p+1)}$ and $k_{t_2}{}^{(p)}$, compute $k_{t_2}{}^{(p+1)}$:

$$k_{t_2}{}^{(p+1)} = \frac{\omega_1^2\big|_{EXP}\left(\rho A\int_0^\ell \phi_1(x)\big|_{ES}^2 dx + m\{\phi_1(x)\}_2^2\big|_{ES\,@\,x=\ell} + J\{\phi_1'(x)\}_2^2\big|_{ES\,@\,x=\ell}\right) - \left(EI\int_0^\ell \phi_1''(x)\big|_{ES}^2 dx + k_{t_1}{}^{(p+1)}\{\phi_1'(x)\}_1^2\big|_{ES\,@\,x=0}\right)}{\{\phi_1'(x)\}_1^2\big|_{ES\,@\,x=a}} \tag{34}$$

This process is repeated until the criterion $\left(\omega_1\big|_{EXP} - \omega_1\big|_{ES}\right)^2 < \tau$ is verified, τ being a given tolerance. For the case ES1 the procedure is limited to one step, where $k_{t_1}{}^{(p+1)} = k_{t_2}{}^{(p+1)}$ is obtained as described in (32).

4 EXPERIMENTAL APPLICATION

As case study setup one uses the Machinery Fault Simulator of figure 1, with $A \approx 1.27 \times 10^{-4}\ \text{m}^2, E = 73\ \text{GPa}$, $I \approx 1.28 \times 10^{-9}\ \text{m}^4$ and $\rho \approx 2.77 \times 10^3\ \text{kgm}^{-3}$. From this setup, our study is focused on the modeling of the beam with an intermediate support in a certain position $a \in [0, \ell]$. The disc one uses is placed at $x = \ell$ and has $m \approx 1.6\ \text{kg}$ and $J \approx 1.5 \times 10^{-3}\ \text{kg.m}^2$. The modal data, namely the natural frequencies were obtained by impact tests on the test equipment. Those results were used as inputs, under the designation $\omega_n\big|_{EXP}$, on the numerical model with the aim of updating the value of the torsional stiffnesses k_{t_j}, besides allowing the comparison of results. All the experiments were performed with the objective of building a straightforward tool for mechanical design.

5 RESULTS AND DISCUSSION

Table 1 shows the results obtained for the first 2 natural frequencies, for the ideal case (SS) as well as for the two considered configurations of the elastically restrained beam (ES1 and ES2). The experimental values of the natural frequencies presented in table 1 are average values obtained from at least three impact tests. As it can be observed, the experimental value for the fundamental frequency does not differ very significantly from the ideal case. However, the experimental value for the second natural frequency is quite different from the obtained for the SS case, justifying the application of a model with elastic supports.

The calculation of k_{t_1} and k_{t_2} has been made for the cases mentioned in section 2.2.2, ES1 and ES2, following the iterative procedure explained in section 3, with the aim of matching the value of the first natural frequency. In order to validate the results obtained for the stiffnesses, one has used them to predict the value of the second natural frequency. Also in table 1, the summary of the obtained results, predictions and relative errors is showed. Therefore, one has for each ES case, the value of the measured natural frequencies, the results of k_{t_1} and k_{t_2} (after a certain number of iterations p), the correspondent predicted values for the second natural frequency and the resulting relative error.

Figure 3 shows the evolution of k_{t_1} and k_{t_2} values and the resulting value of the fundamental frequency, during the iterative procedure for each ES case.

Table 1: Comparison between the theoretical values of the natural frequencies for each case study – SS, ES1 and ES2 – and the experimental results.

$\omega_1\big|_{EXP}$ [Hz]	$\omega_2\big|_{EXP}$ [Hz]	Case #	n.º of Iter. (p_{end})	$\omega_1\big|_\#$ [Hz] (Error [%])	$\omega_2\big|_\#$ [Hz] (Error [%])	k_{t_1} [Nmrad⁻¹]	k_{t_2} [Nmrad⁻¹]
26.023	199.636	SS	-	24.957 (4.1)	72.570 (63.6)	-	-
		ES1	7	26.023 (0.0)	441.739 (121.3)	234.172	234.172
		ES2	6	26.023 (0.0)	200.530 (0.4)	259.483	248.296
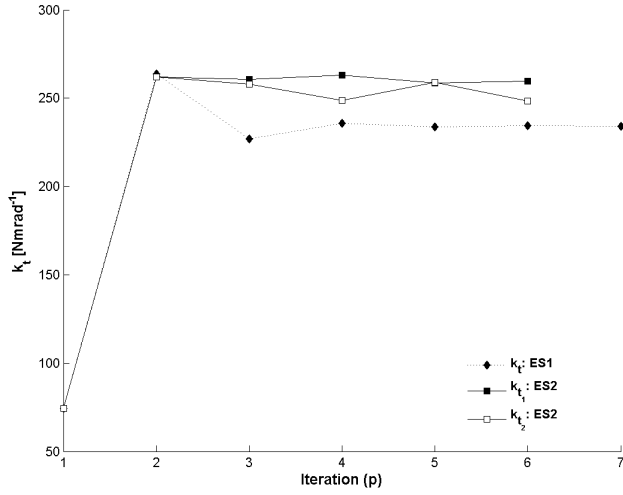
(a)
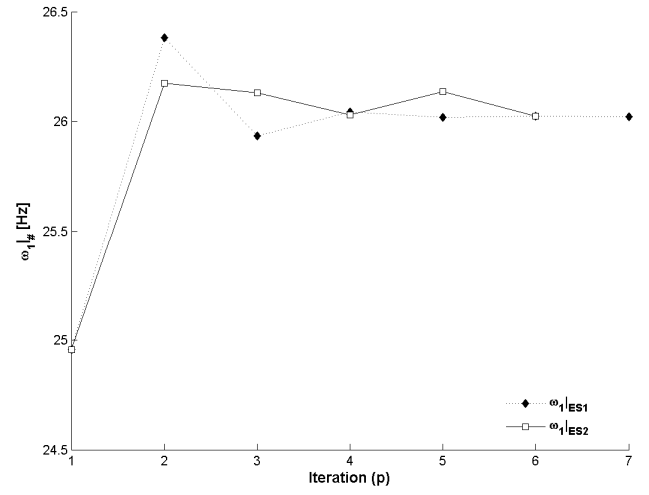
(b)

Figure 3: Evolution of k_{t_j} (a) and $\omega_1\big|_\#$ (b) for the ES case.

With respect to the prediction of the second natural frequency value one should emphasize that the relative error is considerably lower for the result of the ES2 case, even negligible. This fact highlights how important is to consider different stiffnesses coefficients at each support of the beam.

Another significant consideration is the inclusion of mass and inertia elements not just in the energetic terms of the Rayleigh's quotient but also in the mode shapes. Figure 4 intends to illustrate the influence of those elements in the resulting first 4 mode shapes, where solid lines represent the mode shapes obtained for a beam on elastic supports with the free end (case not mentioned in section 2.2) in opposition to the ones obtained for the ES3 case (dashed lines).
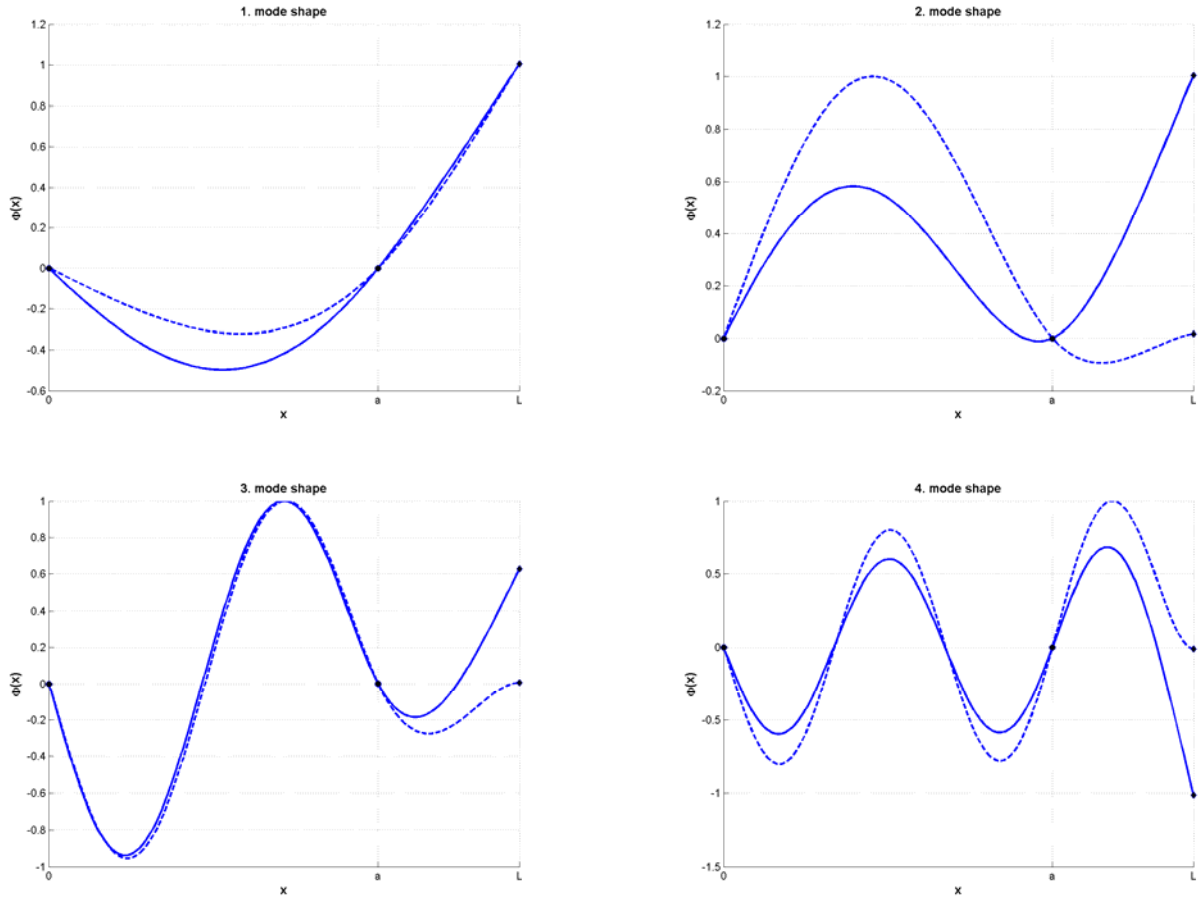
Figure 4: Mode shape deviation due to considering a disc at $x=\ell$: with disc (dashed line) and without disc (solid line).

6   CONCLUSIONS

In order to predict the dynamic behavior of a shaft mounted on elastic supports, with a disc at the free end, a theoretical approach has been developed. From this study, some conclusions can be drawn:

- Modeling a beam on elastic supports is more accurate than assuming it as simply supported. Moreover, assuming that those stiffnesses are different from each other also leads to better results;
- The inclusion of mass and inertia of the disc in the mode shapes has a significant effect on the natural frequencies values;
- It has been proven that after calculating the torsional stiffnesses coefficients based on the experimental value of the first natural frequency it is possible to predict with sufficient accuracy the value of the second natural frequency.

REFERENCES

[1] Meirovitch, L., Fundamentals of vibrations, McGraw-Hill, Boston, 2001, ISBN 0-07-118174-1.

[2] DeRosa, M., Franciosi, C. and Maurizi, M., On the dynamic behaviour of slender beams with elastic ends carrying a concentrated mass, Computers & Structures, Vol. 58, No. 6, pp. 1145-1159, 1996.

[3] DeRosa, M. and Auciello, N., Free vibrations of tapered beams with flexible ends, Computers & Structures, Vol. 60, No. 2, pp. 197-202, 1996.

[4] Auciello, N., Transverse vibrations of a linearly tapered cantilever beam with tip mass of rotary inertia and eccentricity, Journal of Sound and Vibration, Vol. 194, No. 1, pp. 25-34, 1996.

[5] Nallim, L. G. and Grossi, R. O., A general algorithm for the study of the dynamical behaviour of beams, Applied Acoustics, Vol. 57, No. 4, pp. 345-356, 1999.

[6] Maiz, S., Bambill, D. V., Rossit, C. A. and Laura, P., Transverse vibration of Bernoulli-Euler beams carrying point masses and taking into account their rotatory inertia: Exact solution, Journal of Sound and Vibration, Vol. 303, No. 3-5, pp. 895-908, 2007.

[7] Grossi, R. and Albarracn, C., Eigenfrequencies of generally restrained beams, Journal of Applied Mathematics, Vol. 2003, No. 10, pp. 503-516, 2003.

[8] Albarracin, C., Zannier, L. and Grossi, R., Some observations in the dynamics of beams with intermediate supports, Journal of Sound and Vibration, Vol. 271, No. 1-2, pp. 475-480, 2004.

[9] Wu, J.-S. and Chen, D.-W., Bending vibrations of wedge beams with any number of point masses, Journal of Sound and Vibration, Vol. 262, No. 5, pp. 1073-1090, 2003.

[10] Biondi, B. and Caddemi, S., Closed form solutions of Euler-Bernoulli beams with singularities, International Journal of Solids and Structures, Vol. 42, No. 9-10, pp. 3027-3044, 2005.

[11] Biondi, B. and Caddemi, S., Euler-Bernoulli beams with multiple singularities in the flexural stiffness, European Journal of Mechanics - A/Solids, Vol. 26, No. 7, pp. 789-809, 2007.

[12] Elishakoff, I. and Pentaras, D., Apparently the first closed–from solution of inhomogeneous elastically restrained vibrating beams, Journal of Sound and Vibration, Vol. 298, No. 1-2, pp. 439-445, 2006.

[13] Lee, S. Y. and Lin, S. M., Vibration of elastically restrained non-uniform Timoshenko beams, Journal of Sound and Vibration, Vol. 183, No. 3, pp. 403-415, 1995.

[14] Posiadała, Free vibrations of uniform Timoshenko beams with attachments, Journal of Sound and Vibration, Vol. 204, No. 2, pp. 359-369, 1997.

[15] Lin, S. C. and Hsiao, K. M., Vibration analysis of a rotating Timoshenko beam, Journal of Sound and Vibration, Vol. 240, No. 2, pp. 303-322, 2001.